# IMPACT OF OTA NONLINEARITIES ON THE PERFORMANCE OF CONTINUOUS-TIME OTA-C BANDPASS FILTERS

Douglas L. Hiser
*International Microelectronic Products*
2830 N. First St.
San Jose, CA 95134, USA

Randall L. Geiger
*Department of Electrical Engineering*
*Texas A&M University*
College Station, TX 77843, USA

## ABSTRACT

A new technique for predicting actual large-signal frequency responses, including jump resonance, in high-Q bandpass filters constructed from OTAs (operational transconductance amplifiers) and Cs (linear capacitors) is presented. These predictions are a function of the nonlinearities of the OTAs and the Q enhancement of the filter. This approach offers significant advantages over other published techniques: a closed-form expression is obtained which is used to estimate the sensitivity of the nonideal filter parameters to signal amplitude, OTA distortion and Q enhancement and which offers valuable insight into the nonideal operation of the filter. A representative filter structure is discussed which shows close agreement between measured and predicted responses in the presence of both Q enhancement and OTA distortion.

## INTRODUCTION

Active continuous-time filters employing operational transconductance amplifiers (OTAs) are considered a viable means of filtering continuous-time waveforms in a monolithic CMOS technology, particularly in high frequency applications [1]–[4]. The filter characteristics of such architectures are typically adjusted by physically varying the bias current of the input stage of each of the OTAs in a way which compensates for the statistical process variation of the fabricated filter. Unlike filters composed of conventional (voltage-controlled-voltage-source) operational amplifiers which require a large amount of feedback for proper operation, the input port of the OTA is subject to relatively large signal amplitudes, distorting the standard differential pair [5]. In order to reduce this distortion, complex linearization schemes are often applied to the OTA's input stage [6]–[7]. Unfortunately, because of wafer-level statistical process variations and varying bias currents, this strategy falls short of its goal allowing distortion in the OTA to degrade the performance of the continuous-time filter.

Within the last year, two papers have addressed the problem of predicting and simulating the distortion of frequency responses of OTA-C filters due to large excitations [8], [9]. Of these papers [8] is a rigorous analysis technique based on the Volterra series for evaluating the performance of nonideal filters even under multi-tonal excitations. This approach is fairly complex, and is better suited for integration into an existing circuit analysis program. The second paper [9] uses the Tarmy-Ghausi perturbation analysis technique [10] to approximate a filter's performance under stimulus of spectrally pure large signal excitations. Both of these techniques give the designer a method of simulating a nonideal filter's response to large excitations. However, neither of these techniques presented supplies the designer with (a) a closed-form expression summarizing the filter's sensitivity to large excitations; (b) physical insight into the cause of this distortion phenomenon; or (c) a quantitative understanding of the role Q enhancement plays in this issue. In this paper this gap will be bridged, giving the designer a simple technique for quantitatively comparing various OTA-C architectures with respect to over-ordering-induced Q enhancement and OTA-induced nonlinear distortion.

## ANALYSIS

First, a basic technique for modelling the transfer function of the nonideal over-ordered Q-enhanced filter will be presented for a specific high-Q bandpass filter architecture [5], [11]. This structure will be considered throughout this paper. The nonlinear distortion of the OTA will be modelled and incorporated into the nonideal filter transfer function to produce a nonideal amplitude-dependent filter response. From this model, distortion of the frequency response and jump resonance will be simulated and compared to experimental results. Finally, a sensitivity analysis will be performed to quantify the relative impact that the OTA distortion and Q enhancement have on the overall performance of the filter.

### MODELLING

System Transfer Functions: An ideal second-order bandpass circuit is characterized by a transfer function of the form

$$T_{BP}(s) \equiv \frac{V_o(s)}{V_i(s)} = H_{max} \frac{\frac{\omega_o}{Q} s}{s^2 + \frac{\omega_o}{Q} s + \omega_o{}^2}. \quad (1)$$

If parasitic linear capacitors or resistors inherent in the filter structure and the active devices are considered, the actual transfer function will deviate from $T_{BP}(s)$ through both over-ordering and shifts in the parameters $\omega_o$, Q and $H_{max}$. If nonlinearities are also considered, the response of the network will deviate even further from Eq. (1) and the transfer function concept will no longer be defined. The resulting distorted nonlinear filter response becomes both signal and frequency dependent. Throughout this paper, we will use the term "distorted frequency response" or "distorted transfer function" to denote the ratio of the fundamental of the output of a filter to a spectrally pure excitation. The distorted frequency response thus becomes both amplitude and frequency dependent and is strongly a function of both distortion in the OTA and over-ordering of the linearized transfer function. Observe that the distorted frequency response is actually the response measured by many commercial spectrum analyzers. In this paper, emphasis will be placed on accurately modelling the distorted frequency response. Three parameters which characterize the distorted frequency response will be parametrically modelled. These parameters are the distorted or perturbed

$\omega_o$, Q and $H_{max}$ filter parameters, denoted by $\tilde{\omega}_o$, $\tilde{Q}$ and $\tilde{H}_{max}$. Functionally, these parameters correspond to various real and imaginary components of the model distorted transfer function,

$$\tilde{T}_{BP}(j\omega) = \frac{V_o(j\omega)}{V_i(j\omega)} = \tilde{H}_{max} \frac{\frac{\tilde{\omega}_o}{\tilde{Q}} j\omega}{-\omega^2 + \frac{\tilde{\omega}_o}{\tilde{Q}} j\omega + \tilde{\omega}_o^2}, \quad (2)$$

where $\tilde{T}_{BP}(j\omega)$ is the ratio of the fundamental component at the output to the magnitude of a spectrally pure input. In general, the parameters $\tilde{\omega}_o$, $\tilde{Q}$ and $\tilde{H}_{max}$ are dependent on both the input signal amplitude and the frequency $\omega$. They will be defined in such a way that they reduce to the ideal values of $\omega_o$, Q and $H_{max}$ as defined in Eq. (1) as the amplitude goes to zero and as the over-ordering parasitics go to zero.

Tarmy-Ghausi Technique: There are two strategies for defining these nonideal filter parameters in terms of over-ordering. The Tarmy-Ghausi technique models the finite bandwidth of each of the filter components (typically using single or double pole models) and computes an over-ordered transfer function. From this transfer function, the higher-order poles and zeros are eliminated or ignored, resulting in a transfer function in the form of Eq. (2). The nonideal filter parameters are then determined by equating one-to-one each term of the numerators and denominators of these expressions.

Phase-Error Technique: Another technique useful for analyzing high-Q bandpass filters is the phase-error technique. This technique models the finite bandwidth of the filter components as a fixed phase shift over the passband. The nonideal resonant frequency ($\tilde{\omega}_o$) is then defined as the theoretical frequency at which the denominator of the nonideal transfer function becomes purely imaginary. At this frequency ($\omega = \tilde{\omega}_o$), the other nonideal parameters can be determined mathematically. The nonideal filter Q is defined by equating the two denominators and solving for $\tilde{Q}$. Similarly, the nonideal peak gain is defined as the ratio of the numerator to the denominator.

Over-Ordered Model: Of particular concern in most high-Q bandpass filter architectures is the tendency of the Q and peak gain ($H_{max}$) of the fabricated filter to deviate drastically from the design values. This tendency has been directly linked to the finite frequency response of the fabricated OTA and has been modelled in the past with a single- or double-pole model for each OTA. We have developed a simple Q-enhanced model which characterizes this finite frequency response as excess phase ($\theta_p$) included in the $\omega_o^2$ term in the denominator for frequencies in the vicinity of $\omega_o$. In general, this excess phase nonideality shifts a portion of the real component of the fixed $\omega_o^2$ term into the purely imaginary Q-defining component of the denominator, thus affecting the Q and $H_{max}$ characteristics of the filter. This model gives the designer insight into how sensitive the Q enhancement is to excess phase contributed by the OTAs through a closed-form equation predicting this nonideality, and provides the designer with a figure of merit for evaluating OTA designs as well as useful insight into the nature of the Q enhancement characteristic. Finally, the Q enhancement of the filter will also be directly linked to an increase in the sensitivity of the filter to OTA distortion.

OTA Distortion Model: A simple model for the THD characteristics of the OTA can be developed by modelling the distortion characteristic as a shift in power from the fundamental to DC and harmonic components assumed to be outside the passband of the filter.

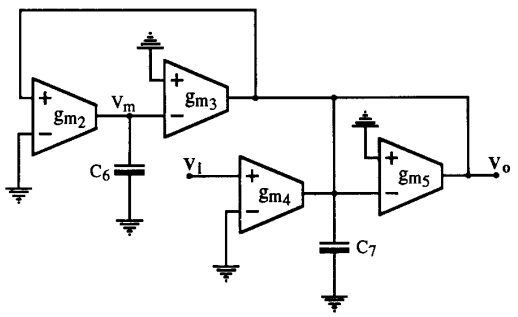


Fig. 1. Circuit schematic of the example high-Q bandpass filter architecture.

This can be viewed as a loss of power in the fundamental. Mathematically, this nonideal distorted transconductance ($\tilde{g}_{m_j}$) is modelled as

$$\tilde{g}_{m_j} = g_{m_j}\,\alpha(|V_j^+ - V_j^-|) = g_{m_j}\sqrt{1 - THD(|V_j^+ - V_j^-|)}, \quad (3)$$

where $g_{m_j}$ represents the ideal OTA transconductance attenuated by $\alpha$ as a function of the differential input signal amplitude across the OTA inputs ($V_j^+$, $V_j^-$). Alternatively, the attenuation can be expressed in terms of a THD function explicitly modelling the total harmonic distortion produced by the $j^{th}$ OTA as a function of its input signal amplitude. This THD function depends on the specific linearization scheme deployed and is typically derived either from experimental measurements or SPICE distortion analysis of the OTA.

## HIGH-Q BANDPASS FILTER EXAMPLE

Consider the high-Q bandpass filter depicted in Fig. 1 and the associated nonideal distorted transfer functions in Eq. (4) which were derived by formally substituting the distorted transconductance of Eq. (3) for each transconductance element of the system's ideal transfer function and including $\theta_p$ which accounts for over-ordering assuming the OTAs are distortion-less.

$$\tilde{T}_{BP}(j\omega) = \frac{\frac{\tilde{g}_{m_4}}{C_7} j\omega}{-\omega^2 + \frac{\tilde{g}_{m_5}}{C_7} j\omega + \left[\frac{\tilde{g}_{m_2}\,\tilde{g}_{m_3}}{C_6\,C_7}\right] e^{j\theta_p}} \approx \frac{\tilde{H}_{max}\frac{\tilde{\omega}_o}{\tilde{Q}} j\omega}{-\omega^2 + \frac{\tilde{\omega}_o}{\tilde{Q}} j\omega + \tilde{\omega}_o^2} \quad (4a)$$

$$\tilde{T}_m(j\omega) \equiv \frac{V_m(j\omega)}{V_i(j\omega)} = \frac{\frac{\tilde{g}_{m_2}\,\tilde{g}_{m_4}}{C_6\,C_7}}{-\omega^2 + \frac{\tilde{g}_{m_5}}{C_7} j\omega + \left[\frac{\tilde{g}_{m_2}\,\tilde{g}_{m_3}}{C_6\,C_7}\right] e^{j\theta_p}} \quad (4b)$$

The parameters contained in the model bandpass transfer function (the right-most expression of Eq. (4a)) can be approximated from the real and imaginary components of the nonideal distorted transfer function (the center expression) via the phase-error analysis technique described earlier. This results in the following closed-form expressions for these nonideal filter parameters, defined in terms of the excess phase ($\theta_p$), the various OTA distortion/attenuation factors ($\alpha$) and the ideal non-over-ordered small-signal filter parameters ($\omega_o$, Q and $H_{max}$).

$$\tilde{\omega}_o \equiv \omega_o \cos\left(\frac{\theta_p}{\sqrt{2}}\right)\sqrt{\alpha(|V_o|)\,\alpha(|V_m|)} \quad (5a)$$

$$\tilde{Q} \equiv Q\frac{\gamma_p}{1 - \rho_c\,\gamma_p} \quad (5b)$$

$$\tilde{H}_{max} \equiv H_{max} \frac{\alpha(|V_i|)}{\alpha(|V_o|)} \frac{1}{1-\rho_c \gamma_p} \quad (5c)$$

where $\rho_c$ (the cross-coupling coefficient) and $\gamma_p$ (the internal peaking factor) are defined as follows:

$$\rho_c \equiv \left. \frac{\mathrm{Imag}\left(\frac{g_{m_2} g_{m_3}}{C_6 C_7}\right)}{\frac{g_{m_5}}{C_7}\omega} \right|_{\omega=\omega_o} = \sin(\theta_p)\, Q \quad (6a)$$

$$\gamma_p \equiv \sqrt{\frac{\alpha(|V_m|)}{\alpha(|V_o|)}} \quad (6b)$$

Basic Algorithm: The magnitude of each of these nonideal parameters can now be computed as a function of the amplitude of the fundamental at each of the filter nodes based on the filter's prior state. From these parameters, a new distorted transfer function and filter response to a given excitation can be determined. By repeating this process and slowly sweeping the excitation frequency, the distorted frequency response of the nonideal system can be accurately modelled. Similarly, by sweeping the amplitude of the excitation at a given frequency up and down during this process, the hysteresis effect which is characteristic of jump resonance can also be predicted. In general, this algorithm takes a series of input signals with varying frequencies and amplitudes, and computes each corresponding output signal amplitude ($|V_{o_k}|$) as a function of the current state of the filter via the following equation:

$$\begin{bmatrix} |V_{o_{k+1}}(j\omega_{k+1})| \\ |V_{m_{k+1}}(j\omega_{k+1})| \end{bmatrix} = \begin{bmatrix} |T_{BP}(j\omega_{k+1}, |V_{i_k}|, \ldots, |V_{o_k}|)| \\ |T_m(j\omega_{k+1}, |V_{i_k}|, \ldots, |V_{o_k}|)| \end{bmatrix} |V_{i_{k+1}}(j\omega_{k+1})| \quad (7)$$

where $\omega_k$ is the frequency of the $k^{th}$ input signal with amplitude $|V_{i_k}|$. It is important that $|V_i|$ and $\omega$ be changed gradually, since Eq. (7) assumes that $|V_{o_{k+1}}| \approx |V_{o_k}|$, $|V_{m_{k+1}}| \approx |V_{m_k}|$ and $|V_{i_{k+1}}| \approx |V_{i_k}|$.

Sensitivity Analysis: Another advantage of this analysis technique is that from Eq. (5) the sensitivity of each of these nonideal filter parameters to variation in the distortion contributed by each of the OTAs can be computed in terms of the amount of Q-enhancement present—giving the designer a closed-form expression for evaluating the relative sensitivity this architecture has to amplitude dependencies. To illustrate this point, these distortion-related sensitivities have been computed in terms of the Q-enhancement factor ($\tau_Q$) and are contained in Table 1. This $\tau_Q$ factor quantifies the amount of small-signal Q-enhancement that is present in the filter and is defined by Eq. (8).

$$\tau_Q \equiv \lim_{|V_i| \to 0} \frac{\tilde{Q}}{Q} = \frac{1}{1-\rho_c} = \frac{1}{1-\sin(\theta_p)\, Q} \quad (8)$$

Table 1. Approximate sensitivities of the various nonideal filter parameters contained in Eq. (5) to the distortion measures THD($|V_i|$), THD($|V_m|$) and THD($|V_o|$) in terms of $\tau_Q$.

| Nonideal Filter Parameter | Sensitivity to THD($\lvert V_i \rvert$) | Sensitivity to THD($\lvert V_m \rvert$) | Sensitivity to THD($\lvert V_o \rvert$) |
|---|---|---|---|
| $\tilde{\omega}_o$ | 0 | $-\frac{1}{4}$ | $-\frac{1}{4}$ |
| $\tilde{Q}$ | 0 | $-\frac{1}{4}\tau_Q$ | $+\frac{1}{4}\tau_Q$ |
| $\tilde{H}_{max}$ | $-\frac{1}{2}\tau_Q$ | $-\frac{1}{4}(\tau_Q - 1)$ | $+\frac{1}{4}(\tau_Q + 1)$ |

## EXPERIMENTAL RESULTS

Distorted Frequency Response: The nonideal "large-signal" frequency response of the high-Q bandpass filter of Fig. 1 was simulated using the "simple" THD model,

$$\mathrm{THD}(|V^+ - V^-|) \equiv 0.658\, |V^+ - V^-| \frac{\%}{V_{rms}}, \quad (9)$$

where $|V^+ - V^-|$ is the rms differential input signal amplitude applied to the various OTAs. This linear model for the OTA distortion was interpolated through a single experimental data point. In Fig. 2, the results of this simulation are contrasted with the experimental results collected on an HP3585a Spectrum Analyzer from the fabricated filter [11]. These results illustrate the ability of this analysis technique to accurately predict distorted frequency responses in the presence of both Q enhancement and OTA distortions. Furthermore, this technique gives the designer useful insight into the performance of the filter, illustrated in Fig. 3 by the dynamic variation of $\tilde{\omega}_o$ as a function of the input signal frequency used in simulating the nonideal frequency response of Fig. 2. Note in Fig. 3 that the peak $\tilde{\omega}_o$ variation of –0.4% could just as easily have been predicted from the sensitivity results of Table 1, assuming THD($|V_o|$) = THD($|V_m|$) = +0.8%.

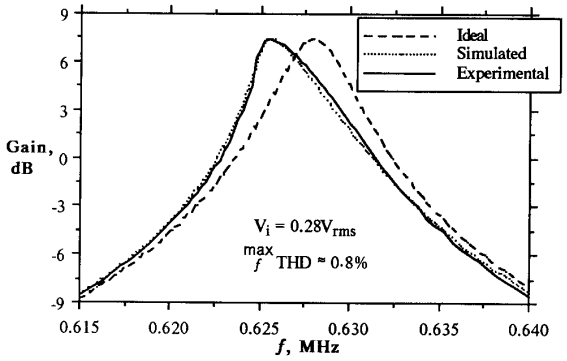


Fig. 2. A comparison of experimental and simulated distorted "large signal" frequency responses for the high Q bandpass filter structure (Fig. 1) with Q≈150 and $\tau_Q$≈2.35. The results shown here were collected and simulated by sweeping the input frequency from left to right while maintaining a fixed amplitude of $0.28V_{rms}$. The ideal response shown here was simulated by eliminating the OTA distortion effects of the nonideal model.

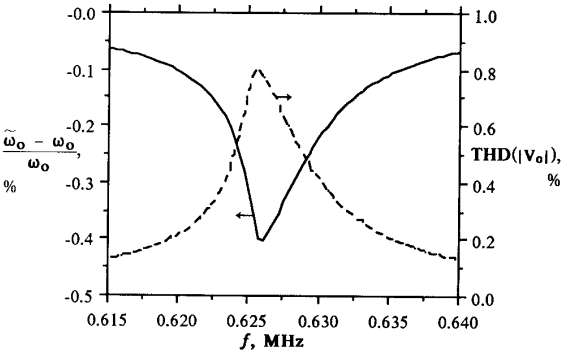


Fig. 3. Simulated $\tilde{\omega}_o$ and THD($|V_o|$) variation associated with the distorted large-signal frequency response contained in Fig. 2.

Jump Resonance: This theory also predicts jump resonance as shown in Fig. 4. In this simulation, a single monotone input signal of frequency slightly lower than the center frequency and of varying amplitude was supplied to the filter characterized in Figs. 2 and 3. In order to encourage jump resonance at this frequency, it is necessary that the sensitivity of $\widetilde{Q}$ to distortion-related perturbations be predominantly positive, indicating that the THD($|V_o|$) is much larger than the THD($|V_m|$). In this situation an increase in input signal amplitude increases $\widetilde{Q}$ and decreases $\widetilde{\omega}_o$. An increase in $\widetilde{Q}$ decreases the filter's gain at this frequency, while a decrease in $\widetilde{\omega}_o$ has the opposite effect and increases the gain. The $\widetilde{\omega}_o$ variation dominates slightly, producing a gradual increase in gain. As the effective center frequency moves towards the input frequency, the impact that the $\widetilde{Q}$ variation has on the gain is reduced. This increases the pace at which the gain increases, and eventually results in an abrupt transition as the effective center frequency snaps to the input signal frequency.

With the signal amplitude at its maximum, the amplitude is decreased causing $\widetilde{\omega}_o$ to increase and $\widetilde{Q}$ to decrease (increasing the effective bandwidth of the filter). Essentially, the lower pass bandedge is to the left of the signal frequency and as the signal amplitude is decreased this bandedge moves slowly towards the signal frequency. Eventually, the signal frequency goes over this bandedge, greatly reducing the output signal level and its associated distortion, and snapping back to the original low distortion curve.

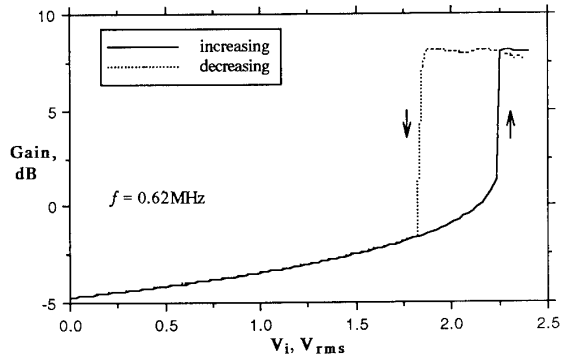


Fig. 4. Typical jump resonance hysteresis effects simulated by the basic theory described in this paper for the high Q bandpass filter of Fig. 1 under stimulus of large signal amplitudes of frequency 0.62MHz. This simulation was performed by first increasing and then decreasing the amplitude of the input signal.

## LIMITATIONS AND EXTENSIONS OF THE ANALYSIS

The analysis scheme presented here has two limitations that should be noted:

(1) It is assumed the harmonics generated by the filter are so small that their contribution to the overall distortion of the filter can in general be neglected.

(2) The current analysis produces a large-signal amplitude-dependent transfer function, thereby limiting the scope of the analysis to the frequency domain and monotone input signals.

Furthermore, the analysis presented here could be expanded to include the following aspects:

(1) The distortion of the OTA could be described as a complex function involving the voltage amplitudes of both the input signal and the output node.

(2) Other filter transfer functions (e.g., lowpass, highpass, etc.) including higher-order structures with a wide range of Qs could be investigated with this technique. This would require the designer to develop an accurate nonideal model of the architecture, including such nonidealities as over-ordering, non-zero output conductance, etc.

## CONCLUSIONS

A new technique for predicting distorted frequency responses, including jump resonance, in high-Q bandpass filter structures is presented as a function of the nonlinearities of operational transconductance amplifiers (OTAs) and the Q enhancement of the filter. The analysis and simulation methodology presented in this paper agrees closely with experimental results, confirming the validity of the basic theory. This analysis offers significant advantages over other published techniques by offering practical insight into the nonideal performance of the filter, in terms of parameters which directly characterize both the frequency response and distortion of the OTA.

## REFERENCES


[1] C. S. Park and R. Schaumann, "Design of a 4MHz Analog Integrated CMOS Transconductance-C Bandpass Filter," *IEEE Journal of Solid-State Circuits*, vol. SC-23, Dec. 1988, pp. 987–996.

[2] E. Sánchez-Sinencio, R. L. Geiger and H. Nevárez-Lozano, "Generation of Continuous-Time Two-Integrator-Loop OTA Filter Structures," IEEE Trans on Circuits and Systems, vol. CAS-35, no. 8, Aug. 1988, pp. 936–945.

[3] A. Urbas and J. Osiowski, "High-Frequency Realizations of C-OTA Second-Order Active Filters," in *IEEE Proc. of Int. Symp. on Circuits and Systems*, May 1982, pp. 1106–1109.

[4] H. S. Malvar, "Electronically Controlled Active-C Filters and Equalizers with Operational Transconductance Amplifiers," *IEEE Trans on Circuits and Systems*, vol. CAS-31, no. 7, July 1984, pp. 645–649.

[5] R. L. Geiger and E. Sánchez-Sinencio, "Active Filter Design Using Operational Transconductance Amplifiers: a Tutorial," *IEEE Circuits and Devices Mag.*, vol. 1, March 1985, pp. 20–32.

[6] A. Negungadi and T. R. Viswanathan, "Design of Linear CMOS Transconductance Elements," *IEEE Trans on Circuits and Systems*, vol. CAS-31, no. 10, Oct. 1984, pp. 891–894.

[7] C. S. Park and R. Schaumann, "A High-Frequency CMOS Linear Transconductance Element," IEEE Trans on Circuits and Systems, vol. CAS-33, no. 11, Nov. 1986, pp. 1132–1138.

[8] S. Szczepanski and R. Schaumann, "Effects of Weak Nonlinearities in Transconductance-Capacitor Filters," in *IEEE Proc. of Int. Symp. on Circuits and Systems*, May 1989, pp. 1055–1058.

[9] P. Bowron and H. M. Dahir, "Modelling of Nonideal Active Devices in Continuous-Time OTA-C Filters," in *Proc. of European Conference on Circuit Theory and Design*, Sept. 1989, pp. 128–131.

[10] R. Tarmy and M. S. Ghausi, "Very High-Q Insensitive Active-RC Network," *IEEE Trans. on Circuit Theory*, vol. CT-17, Aug. 1970, pp. 358–366.

[11] K.-H. Loh, D. L. Hiser, W. J. Adams and R. L. Geiger, "A Robust Digitally Programmable and Reconfigurable Monolithic Filter Structure," in *IEEE Proc. of Int. Symp. on Circuits and Systems*, May 1989, pp. 110–113.